

Low gap superconducting single photon detectors for infrared sensitivity

S. N. Dorenbos,^{a)} P. Forn-Díaz, T. Fuse, A. H. Verbruggen, T. Zijlstra, T. M. Klapwijk, and V. Zwiller

Kavli Institute of Nanoscience, TU Delft, 2628CJ Delft, The Netherlands

(Received 7 February 2011; accepted 23 May 2011; published online 20 June 2011)

The quantum efficiency of NbN and NbTiN superconducting single photon detectors drops with decreasing photon energy. A lower gap material would enable single photon detection deeper in the infrared. We have fabricated a NbSi detector and compare its characteristics with a NbTiN device. NbSi ($T_C \approx 2$ K) has a smaller superconducting gap than NbTiN or NbN ($T_C \approx 15$ K). We measure the detection efficiency for a wavelength range from 1100 to 1900 nm. In this range the NbSi detector shows a 10-fold increase in relative efficiency with respect to the NbTiN detector. © 2011 American Institute of Physics. [doi:10.1063/1.3599712]

Superconducting single photon detectors (SSPDs) made from a NbN or NbTiN nanowire are sensitive to single photons.^{1,2} These detectors show a low dark count rate, low timing jitter (60 ps),³ short dead time (10 ns),¹ and are already used in various experiments ranging from quantum key distribution⁴ and entanglement experiments⁵ to time of flight measurements,⁶ characterization of optical quantum dots,⁷ and near-field sensing of surface plasmon polaritons.⁸ The detector usually consists of a long (~ 500 μm) superconducting nanowire with a width of ~ 100 nm, and a thickness ~ 5 nm. The operation principle is based on the transition from the superconducting state to the normal state of a segment of the nanowire after absorption of a single photon. Their efficiency is moderate (up to 30%) in the visible part of the spectrum and drops considerably for wavelengths above 1 μm . Efficient single photon detectors in the infrared ($\lambda > 1$ μm) will enable quantum optics experiments with single photon sources emitting in the infrared (i.e., low gap semiconductor or carbon nanotube quantum dots) and study of intraband transitions. One approach to increasing the efficiency in the infrared is the use of optical cavities.^{3,9} In this way the absorption probability is increased (up to 80%) but this approach is not helpful when the photon energy is insufficient to induce a detection event. In order to have detectors as sensitive in the near infrared as in the visible part of the spectrum, we have fabricated SSPDs of amorphous NbSi. We compare NbTiN and NbSi by measuring the quantum efficiency (QE) as a function of wavelength.

There is no complete theory for the microscopic detection principle of photons with SSPDs. However it is generally believed that the energy of a photon $E_{ph} = h \times \nu \approx 1$ eV causes breaking of Cooper pairs with a superconducting band gap energy of $E_g \sim k \times T_c \approx 5$ meV (for NbTiN). The increased number of quasiparticles leads to a finite resistance in a section of the nanowire, inducing a detection event. With decreasing photon energy, fewer Cooper pairs are broken and the QE of the SSPD drops. A lower E_g yields a higher E_{ph}/E_g ratio and more Cooper pairs per photon are broken, leading to a higher QE. SSPDs made of NbSi have a critical temperature of ~ 2 K, meaning that the superconducting gap is approximately 10 times lower than NbTiN (and NbN) with

$T_c \sim 15$ K.¹⁰ In addition, NbSi has a high resistivity, necessary to make efficient SSPDs.¹¹

Fabrication of NbSi SSPDs is comparable to the fabrication of NbTiN SSPDs.² First a 10 nm layer $\text{Nb}_{0.48}\text{Si}_{0.52}$ is cosputtered from a Nb (dc) and a Si (rf) target on oxidized silicon. The sheet resistance is typically 262 Ω/sq . A film of this thickness and composition has a critical temperature of approximately 2 K. Nb/AuPd contacts are lithographed using liftoff and the NbSi wire is etched with reactive ion etching in a gas mixture of SF_6 and He. The wire is 160 nm wide and 90 μm long, a scanning electron microscope picture of a device similar to the ones used in the experiment is shown in Fig. 1(a). The NbTiN nanowire has a width of 100 nm and a length of 500 μm .

A NbSi detector and a NbTiN detector are cooled down in a ^3He cryostat, equipped with a multimode optical fiber. The measurement temperature is 300 mK. To directly compare the sensitivity of NbSi with NbTiN, we place the two detectors besides each other and an optical fiber is mounted

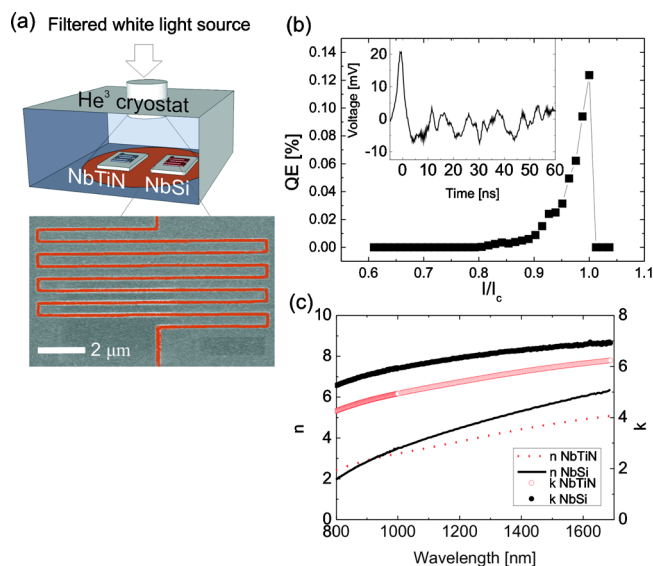


FIG. 1. (Color online) (a) Schematic of the setup and (colored) scanning electron microscope picture of the NbSi SSPD. The box represents the ^3He cryostat with an optical fiber feedthrough. A NbTiN and a NbSi detector are mounted besides each other such that both detectors are illuminated equally. (b) QE of the NbSi detector for $\lambda = 1700$ nm. (Inset) Typical detection pulse after amplification. (c) Measured optical constants of NbSi.

^{a)}Electronic mail: s.n.dorenbos@tudelft.nl.

above the detectors such that the spot simultaneously illuminates both detectors with approximately the same intensity [see Fig. 1(a)]. A supercontinuum white light source filtered by a monochromator is used as the excitation light source. A long pass filter at 1100 nm blocks second orders produced by the monochromator. The output of the monochromator is calibrated with a spectrometer and a full width half maximum of the linewidth of ≤ 1.6 nm is measured. We have confirmed that no second order was present. The SSPDs are biased with dc current and the output pulses are amplified (gain +30 dB) and read out with either a pulse counter or an oscilloscope. The critical current of the NbSi SSPD was $2.2 \mu\text{A}$ ($0.9 \cdot I_c$), implying a critical current density of $1.4 \times 10^5 \text{ A/cm}^2$ ($0.63 \cdot I_c$). The QE under illumination with 1700 nm light is shown in Fig. 1(b). As expected, the QE exponentially increases with current. A typical photon detection pulse is shown in the inset of Fig. 1(b). The pulse length (1 ns) is limited by the bandwidth of our amplifiers (0.01–1 GHz). Given the relatively low kinetic inductance of our device (~ 50 nH), the reset time of the device is shorter than 1 ns. The absorption efficiency is determined by the optical constants of the material, in particular, the complex index of refraction (k).¹² We have measured the optical constants of NbSi and NbTiN with an ellipsometer. This is shown in Fig. 1(c), and it can be seen that the complex index of refraction of NbSi is comparable to NbTiN, which means that the absorption efficiency will be similar.

In Fig. 2(a), the count rates for the NbTiN detector and the NbSi detector are shown as a function of wavelength. The detectors were current biased at $10 \mu\text{A}$ and $1.4 \mu\text{A}$, respectively. We have observed that latching occurs if a higher bias current for the NbSi detector was used. We attribute this latching to the low kinetic inductance of the device, preventing the detector from cooling down and returning to the superconducting state, as the current in the device returns too fast.¹³ Increasing the length of the wire will increase the kinetic inductance, which will allow biasing the detector closer to the critical current and increase the active area. We measure a dark count rate of less than 1 count/s for both detectors. For each point the integration time was 30 s. By measuring the power, we also calculated the QE for the wavelengths 1100 to 1700 nm. Figure 2(a) shows that the QE drops exponentially with increasing wavelength for both detectors. Using $\log(\text{QE}) = -k \cdot \lambda$, a linear fit gives a slope of $k_{\text{NbSi}} = 2.67(0.30) \cdot 10^{-3} \text{ nm}^{-1}$ for NbSi and $k_{\text{NbTiN}} = 7.70(0.29) \cdot 10^{-3} \text{ nm}^{-1}$ for NbTiN. This shows that the degradation in efficiency with increasing wavelength is three times slower for NbSi compared to NbTiN. We note that the absolute efficiency of the NbSi detector can be improved by optimizing the geometry of the device.

We have also measured the count rate as a function of power. This is shown in Fig. 2(b) for a wavelength of 1400 and 1800 nm. We plot the NbSi count rate as a function of the NbTiN count rate and fit the data linearly in log-log scale. It has been shown that SSPDs made of NbTiN are single photon detectors for (near) infrared wavelengths.⁷ We confirmed in a separate measurement that the count rate as a function of power of the NbTiN SSPD at $\lambda = 1400$ nm is linear, a clear indication of single photon detection. The slopes of the fit in Fig. 2(b) correspond to 0.95(0.27) and 0.91(0.16), which indicates a linear power dependence. We conclude that the NbSi SSPD is also a single photon detector.

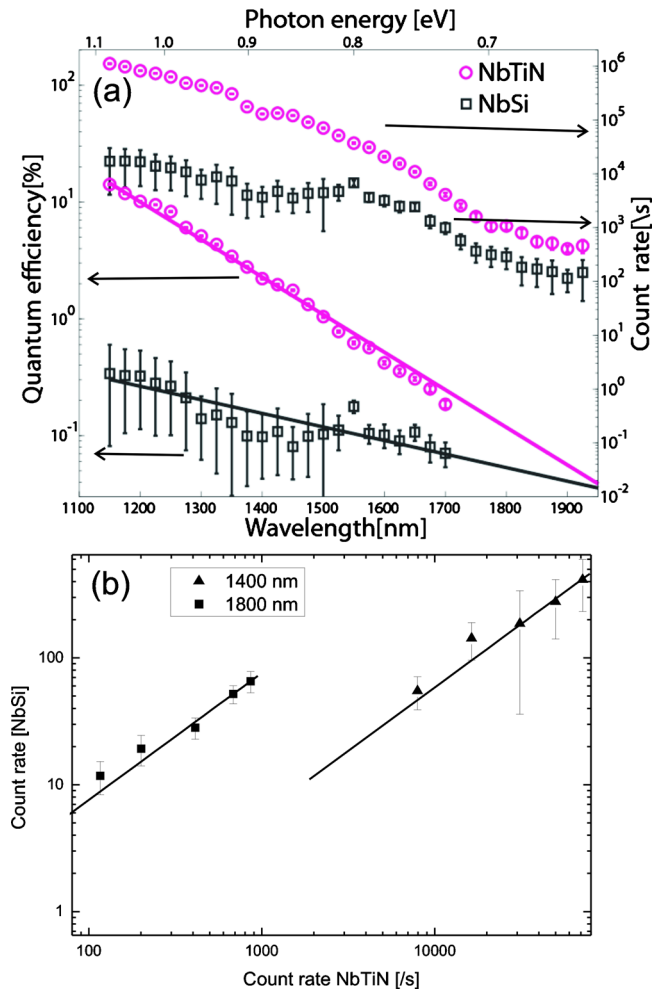


FIG. 2. (Color online) (a) Count rates and QE for the NbTiN (circles) and NbSi (squares) detector. The solid lines through the QE measurements are exponential fits. (b) NbSi count rate as a function of NbTiN count rate for $\lambda = 1400$ nm and $\lambda = 1800$ nm at different powers. The slope in the exponential plot is 0.95(0.27) and 0.91(0.16), for $\lambda = 1400$ nm and $\lambda = 1800$ nm respectively, close to linear.

Figure 3 shows the enhancement in sensitivity for longer wavelengths by plotting the ratio of the count rates as shown in Fig. 2(a) of NbSi and NbTiN. As the ratio increases for longer wavelength it clearly shows the relative improvement of NbSi over NbTiN. The enhancement is more than 10-fold at a wavelength $\lambda = 1900$ nm with respect to $\lambda = 1100$ nm.

In conclusion, we have fabricated and tested NbSi SSPDs. These detectors have a smaller superconducting band

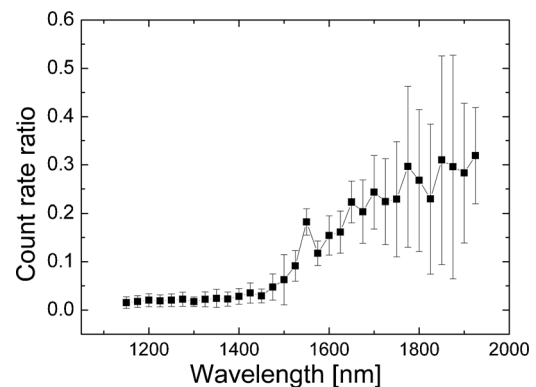


FIG. 3. Count rate ratio of NbSi to NbTiN vs photon wavelength.

gap compared to NbTiN detectors, making them more sensitive for infrared wavelengths. We have compared the relative sensitivity with NbTiN detectors for different wavelengths and observed an enhancement by an order of magnitude over a wavelength range from 1100 nm to 1900 nm. By improving the geometry of the NbSi detector and fiber coupling it,³ a high system detection efficiency for single photons at infrared wavelengths can be achieved.

The authors acknowledge Gilles Buchs and Esteban Bermudez Ureña for setting up the white light source and Professor Karl K. Berggren for discussions. S.N.D. and V.Z. acknowledge funding from FOM. P.F.-D. acknowledges funding from the Dutch NanoNed program and the EU projects EuroSQIP and CORNER.

¹G. N. Gol'tsman, O. Okunev, G. Chulkova, A. Lipatov, A. Semenov, K. Smirnov, B. Voronov, A. Dzardanov, C. Williams, and R. Sobolewski, *Appl. Phys. Lett.* **79**, 705 (2001).

²S. N. Dorenbos, E. M. Reiger, U. Perinetti, V. Zwiller, T. Zijlstra, and T. M. Klapwijk, *Appl. Phys. Lett.* **93**, 131101 (2008).

³M. G. Tanner, C. M. Natarajan, V. K. Pottapenjara, J. A. O'Connor, R. J. Warburton, R. H. Hadfield, B. Baek, S. Nam, S. N. Dorenbos, E. Bermudez Urena, T. Zijlstra, T. M. Klapwijk, and V. Zwiller, *Appl. Phys. Lett.*

96, 221109 (2010).

⁴H. Takesue, S. W. Nam, Q. Zhang, R. H. Hadfield, T. Honjo, K. Tamaki, and Y. Yamamoto, *Nat. Photonics* **1**, 343 (2007).

⁵M. Halder, A. Beveratos, N. Gisin, V. Scarani, C. Simon, and H. Zbinden, *Nat. Phys.* **3**, 692 (2007).

⁶R. E. Warburton, A. McCarthy, A. M. Wallace, S. Hernandez-Marin, R. H. Hadfield, S. W. Nam, and G. S. Buller, *Opt. Lett.* **32**, 2266 (2007).

⁷S. N. Dorenbos, H. Sasakura, M. P. van Kouwen, N. Akopian, S. Adachi, N. Namekata, M. Jo, J. Motohisa, Y. Kobayashi, K. Tomioka, T. Fukui, S. Inoue, H. Kumano, C. M. Natarajan, R. H. Hadfield, T. Zijlstra, T. M. Klapwijk, V. Zwiller, and I. Suemune, *Appl. Phys. Lett.* **97**, 171106 (2010).

⁸R. W. Heeres, S. N. Dorenbos, B. Koene, G. S. Solomon, L. P. Kouwenhoven, and V. Zwiller, *Nano Lett.* **10**, 661 (2010).

⁹K. M. Rosfjord, J. K. W. Yang, E. A. Dauler, A. J. Kerman, V. Anant, B. M. Voronov, G. N. Gol'tsman, and K. K. Berggren, *Opt. Express* **14**, 527 (2006).

¹⁰T. Matsunaga, H. Maezawa, and T. Noguchi, *IEEE Trans. Appl. Supercond.* **13**, 3284 (2003).

¹¹A. J. Annunziata, O. Quaranta, D. F. Santavicca, A. Casaburi, L. Frunzio, M. Ejrnaes, M. J. Rooks, R. Cristiano, S. Pagano, A. Frydman, and D. E. Prober, *J. Appl. Phys.* **108**, 084507 (2010).

¹²V. Anant, A. J. Kerman, E. A. Dauler, J. K. W. Yang, K. M. Rosfjord, and K. K. Berggren, *Opt. Express* **16**, 10750 (2008).

¹³A. J. Kerman, J. K. W. Yang, R. J. Molnar, E. A. Dauler, and K. K. Berggren, *Phys. Rev. B* **79**, 100509 (2009).